RSC Advances

ROYAL SOCIETY OF CHEMISTRY

www.rsc.org/advances

RSC Advances

RSCPublishing

PAPER

Facile formation of micro-crater structure for light scattering in quasi-solid state dye-sensitized solar cells

Cite this: DOI: 10.1039/x0xx00000x

Received 00th January 2014,
Accepted 00th January 2014

DOI: 10.1039/x0xx00000x

www.rsc.org/

Dae Man Han,[a] Kwan-Woo Ko,[b] Chi-Whan Han [*b] and Youn Sang Kim [*ac]

Herein, we introduced the hierarchical micro-porous TiO_2 photo-anode with optimal morphology tailored for gel-type electrolyte DSSCs. To prepare a micro-crater structure, acetylene-black was blended into the TiO_2 paste, thereafter evaporated at high temperature sintering process. The formation of micro-crater structure with optimal morphology improved the light scattering effect without additional light scattering layer, in addition, provided wide entrance for fast and complete electrolyte infiltration into the TiO_2 film. Full contact between the TiO_2 film and the gel-type electrolyte by the micro-crater structure improved the performance of the DSSCs compared to the DSSCs without micro-crater structure. Photo-conversion efficiency of the DSSC using this method was enhanced from 7.9 % to 8.7 %, while maintaining a high stable efficiency in 300 hours stability test.

Introduction

Dye-sensitized solar cells (DSSC) are attracting widespread interests due to no hazardous structure materials for environment, the possibility of aesthetic design for differentiation, facile fabrication process, and high photoelectric conversion efficiency among organic solar cells.[1] A typical DSSC consists of a dye-adsorbed TiO_2 photo-anode and a platinum counter electrode with a liquid-type electrolyte containing I^-/I_3^- redox couple, which is used to fill in between the two electrodes.[2] A lot of efforts have been devoted to improving the performance of DSSCs by increasing the energy conversion efficiency with advanced dyes and improving the light harvesting efficiency with more charge transport in the TiO_2 photo-anode films or less hole-electron recombination at the interface between the photo-anode and the electrolyte. Recently reported advanced sensitized dyes have shown that the porphyrin dye and organic-inorganic hybrid perovskites can be better alternatives for a commercialized ruthenium dye. [3, 4] As a new research in the TiO_2 photo-anode films, the advantages of the doping method such as K-doping, Ta-doping, and Sn-doping have been introduced. [5-7] Diverse hard-template method, soft-templating synthesis method, solvothermal treatment method, and rapid microwave synthesis method were reported to enhance the light harvesting efficiency by the modification of TiO_2 film morphology [8-14]

Meanwhile, as a crucial part of DSSCs, the liquid-type electrolytes are conventionally used materials by many researchers as ionic conducting layers. The high photoelectric conversion efficiency of liquid-type electrolytes is attributed to the high ionic conductivity which comes from; 1. high mobility of redox couple in solvent medium and 2. low contact resistance between TiO_2 photo-anode film and electrolyte by fast and complete infiltration process. On the other hand, liquid-type electrolyte cannot avoid the problem of leakage from the cell by the incomplete sealing or by the saturation vapor pressure at high temperature even the complete sealing.[15] Furthermore, the high fluidity of liquid type electrolytes induces the easy segregation of sensitizing dye from the TiO_2 nanoparticles to the liquid type electrolyte medium.[16]

UV-cured polymer gel electrolytes have more stability and less charge recombination than liquid type electrolytes at room temperature by cross-linked polymer network. DSSCs using UV-cured polymer gel electrolytes have shown even better performance than DSSCs with liquid type electrolytes at high temperature due to the improved ionic mobility.[17] There was an effort to enhance the performance of DSSCs using UV-cured polymer gel electrolytes at room temperature by the introduction of additional nano-gel type electrolyte between the electrolyte and the counter electrode as a high charge transport layer. [18] Otherwise, there has been less effort to tailor the morphology of TiO_2 photo-anode considering the efforts for gel-type electrolyte DSSCs. Normally, additional light scattering layers are used on dense TiO_2 nanoparticle photo-anode films to get higher light harvesting efficiency. However, despite the cumbersome additional process of double layer TiO_2 film, the light harvesting efficiency is less than hierarchical micro-porous structure or multi-layer film. Besides, the

infiltration process of gel-type electrolyte into a complex TiO_2 film takes long time and gives rise to high contact resistance in DSSC fabrication.

For effective light harvesting in DSSCs, hierarchical micro-porous nanocrystalline TiO_2 films were introduced via hard- and soft-templating routes. [19] The hard-templating synthesis is commonly used to fabricate ordered three-dimensional (3D) TiO_2 porous structures with crystalline framework, high specific surface area, and tailored pore structure. This templating route involves the use of colloidal particles, polymeric beads, and anodic alumina membranes, thereafter, these templates would be removed to generate unique porous materials. The soft-templating synthesis involves the use of organic or polymeric surfactants which self-assemble into a diversity of supermolecular structures, including spherical micelles, hexagonal rods, lamellar, and other structures in solution, which are used as soft templates to tune the structure and size of pores in TiO_2 materials. [13] Use of the hierarchical micro-porous TiO_2 films had the merits of improved light scattering effect for enhanced performance of DSSCs. In addition, the large pin holes on the surface improved the infiltration process of gel-type electrolyte into the TiO_2 films. However, achieving both purposes simultaneously with simple fabrication method to facilitate micro-crater structure for wide channel of gel-type electrolyte and nano-pores for light scattering effect are great challenges until now.

In the present study, we exerted ourselves to find an optimal hierarchical TiO_2 photo-anode morphology tailored for the gel-type electrolyte DSSCs by simply adding high temperature volatile material in the TiO_2 paste without using cumbersome hard or soft template. To prepare a micro-crater structure, acetylene-black (hereafter referred to as AB) was blended into the TiO_2 paste, thereafter, evaporated at high temperature of sintering process. Sensitized dye was adhered onto the TiO_2 surface, and then gel-type electrolyte was infiltrated into the micro-crater shaped pores in the TiO_2 film. (Scheme. 1) To find the optimal light scattering condition in mcro-crater structures, the changes of optical properties of the TiO_2 photo-anode films according to the formation of hierarchical micro-crater morphology by the addition and evaporation of AB at high temperature were analyzed using spectrophotometer. Also, the photovoltaic performance and long-term stability of the prepared DSSCs incorporating double layer gel-type electrolyte were studied using solar simulator and IPCE measurement system. This method demonstrated 8.7 % photo-conversion efficiency without using additional light scattering layer, which is around 10% higher than the method fabricating TiO_2 film without adding AB in the TiO_2 paste.

Experimental

Synthesis of TiO_2 nanoparticles and pastes

TiO_2 nanoparticles were synthesized by using the hydrothermal method. [6, 7] Tetrabutyl titanate (10 mL), butanol (60 mL), acetone (10 mL), and acetic acid (10 mL) were mixed. A mixture of butanol (40 mL) and distilled water (3 mL) was then added to the above solution, followed by stirring for 1h and the hydrothermal process at 240 ^oC for 6 hours in an autoclave. The mixture was cooled at room temperature and enriched using a rotary-evaporator in 13 % TiO_2 colloid.

TiO_2 pastes (hereafter referred to as Normal TiO_2 pastes) were prepared by the combustion process using the TiO_2 colloid for the starting material. Ethylene carbonate was added for the binder, and terpineol for the solvent of the TiO_2 colloidal solution, followed by a mixing process using a paste blender. Then, to facilitate a formation of micro-crater structure on the TiO_2 photo-anode films, TiO_2 pastes containing AB (hereafter referred to as AB TiO_2 pastes) were prepared using a paste-blending method in the reference. [20]

Preparation of TiO_2 photo-anode films

To compare the optical properties between the TiO_2 films with (referred to as AB TiO_2 film) and without AB (referred to as Normal TiO_2 film), both TiO_2 pastes were screen printed onto the FTO glass (TEC 8/2.3mm, 8 Ω/sq, Pilkington) in a total area of 100 × 100 mm^2 and then sintered at temperatures of 200 ℃, 450 ℃, and 550 ℃ respectively in ambient air using a muffle furnace.

The transmittance, opacity, and haze of the TiO_2 photo-anodes were measured by transmittance mode, and the diffuse reflectance, and whiteness index of the TiO_2 photo-anodes were measured by reflection mode using a UV-vis spectrophotometer (CM-5 Konica Minolta, Japan) and analyzed using a color data software (SpectraMagic NX Ver.2.1 Konica Minolta, Japan).

Synthesis of electrolytes

Liquid-type electrolytes were prepared by dissolving 0.05M I_2, 0.1M LiI, 0.48M TBP, 0.12M NaSCN, and 0.6M BMII in methoxypropionitrile.

UV-cured polymer gel type electrolytes were prepared by the addition of UV-curable polyurethane acrylate in the liquid-type electrolyte at 12:10 weight ratio with 5 wt% photo initiator in the total solution.

Nano-gel type electrolytes were prepared by the addition of 7 wt% fumed silica nanoparticles in the liquid-type electrolyte as previously reported. [18]

Fabrication of the DSSCs

For the fabrication of the DSSCs, TiO_2 photo-anode films were prepared by the screen printing method with aperture area of 0.2 cm^2 and then sintered at 550 ^oC for 30 minutes. Dye adsorption was carried out by dipping the TiO_2 photo-anode films into 4 × 10^{-4} M t-butanol/acetonitrile (Merck, 1:1) solution of the standard ruthenium dye (N719, Solaronix) for 48 hours at 25 ^oC. In case of double layer gel-type electrolyte, firstly the UV-cured polymer gel type electrolyte was coated on the TiO_2 photo-anode films and then the nano-gel type electrolyte was coated later. Counter electrodes were prepared by dropping the 10 mM hydrogen hexachloroplatinate (IV) hydrate (99.9%, Aldrich) in a 2-propanol solution onto the transparent FTO glass and sintering at 400 ^oC for 30 minutes.

The two electrodes were assembled and separated using thermal adhesive polymer film (Surlyn, thickness 60 μm).

Photovoltaic characterization of the DSSCs

The photovoltaic properties of the prepared DSSCs were measured using a lamp with air mass 1.5G filter as light source in a solar simulator and an exposure control instrument (Newport). The light intensity was adjusted with a reference Si cell (Fraunhofer Institute for Solar Energy System). Photovoltaic performance was characterized by V_{oc}, J_{sc}, and FF (fill factor), and the overall photo-conversion efficiency was characterized using the current density-voltage (J-V) curve.

Incident-photo-to-current efficiencies (IPCE) were measured by the illumination of the prepared DSSCs with a xenon arc light sources through a filter monochromator and optical chopper at 2 Hz under bias light (Newport).

For the stability test under continuous light illumination, the prepared DSSCs were irradiated at open circuit state using a xenon arc lamp at 1 sun condition in an ambient temperature (McScience). Then, the photo-conversion efficiency was characterized periodically.

Results and discussion

To find the optimal heat treatment condition of the AB TiO_2 film prepared as above procedure, optical properties were measured by spectrophotometer. Figure 1(a) shows the transmittance and opacity of the TiO_2 photo anode films including 1.0 wt% AB. These TiO_2 photo anode films were heat treated at 200 and 450 ^oC for 60 minutes, and 550 ^oC for 5 minutes. Transmittance was observed to be near zero at 200 ^oC indicating no evaporation of AB. Transmittance of 35% at 450 ^oC was attributed to the partial evaporation of AB. Maximum transmittance of 67% at 550 ^oC indicates that nearly pure white color was obtained from the almost full decomposition of AB.

In this research, opacity was measured as a parameter for scattering efficiency of visible light due to the formation of hierarchical micro-porous structures in the TiO_2 photo-anode films. The difference between the refractive index of the anatase crystalline TiO_2 films (R.I. 2.55) and the air (R.I. 1) is large enough to provide a diffuse reflectance and opacity by the light-scattering. Opacity in optics is the measure of impenetrability to electromagnetic radiation, especially visible light, also termed as a mass attenuation coefficient or a mass absorption coefficient. In more special condition, if a beam of light with frequency, ν, travels through a medium with constant opacity value, Kν, and constant mass density value, ρ, then the intensity will be reduced with distance, x, according to the formula

$$I(x) = I_0\ e^{-K\nu\rho x}$$

where, x is the distance of the light which has travelled through the medium, $I(x)$ is the intensity of light remaining at distance x, and I_0 is the initial intensity of light, at x=0.

Opacities of the AB TiO_2 photo-anodes were measured after different heat treatment conditions. The opacity value could not be measured after 200 ^oC heat treatment due to no visible light transmission by the remaining organic materials and AB. The opacity value of 85 % after 450 ^oC heat treatment was attributed to partial evaporation of AB resulting in partial absorption and partial scattering of visible light. The maximum opacity value of 98 % after 550 ^oC heat treatment was attributed to nearly full decomposition of AB which facilitated formation of hierarchical micro-crater structure on TiO_2 photo anode film.

In order to find an optimized heat treatment time at selected temperature, AB TiO_2 photo anode films were prepared using different heat treatment times of 30 and 50 minutes at the optimal heat treatment temperature of 550 ^oC. The maximum transmittance value of 68 % was obtained at 30 minutes heat treatment time by the more complete evaporation of AB. This result also confirmed that the more complete evaporation of AB has facilitated more effective light scattering structure. On the other hand, excess heat treatment up to 50 minutes has been proven too long to obtain an effective structure, while exhibiting the lower transmittance of 66 % and the lower opacity value of 95 % due to the excess heat treatment and loss of light scattering effect in the TiO_2 photo anode film. Generally, the thickness of TiO_2 film decreases according to heat treatment time improving the connectivity between the TiO_2 nanoparticles. However, this increase of density in AB TiO_2 photo-anode films induces decrease of nano- and micro-pores facilitated by the evaporation of AB.

The transmittance and the opacity values shown above supported that AB was evaporated completely under the optimized heat treatment conditions facilitating the formation of effective hierarchical micro-crater TiO_2 photo-anode films for light scattering effect. To compare the optical properties variable to the wavelengths of the visible light, transmittance and diffuse reflectance were measured between the TiO_2 photo anode films without and with AB to understand the wavelength range of the light scattered by the effective formation of hierarchical micro-crater structure on the TiO_2 nano-crystalline frame.

Figure 2(a) shows the light transmittances in accordance with a wavelength of the bare FTO glass, Normal TiO_2 films, and AB TiO_2 films. Light transmittances at around 360 nm wavelength are near zero in case of both Normal and AB TiO_2 films due to the ultra violet light region absorbance of the TiO_2 materials, while bare FTO glasses without TiO_2 films exhibit rather higher light transmittances. Light transmittances are recovered in between 400 nm and the visible light regions relying on the thickness and light scattering effect of the Normal TiO_2 films, however, the transmittance of the AB films does not reach the analogous level of Normal films even with only one time coating thicknesses. Figure 2(b) shows the diffuse reflectance in accordance with a wavelength of the bare FTO glass, Normal TiO_2 films, and AB TiO_2 films. Diffuse reflectance at around 360 nm wavelength is near zero in case of the both Normal and AB TiO_2 films, which confirms that ultra violet light region

absorptions by TiO_2 materials are dominant in that wavelength region. Peak diffuse reflectance wavelengths were found at around 400 nm in both TiO_2 films, in the meanwhile bare FTO glasses exhibited no diffuse reflections. Furthermore, AB films have shown rather higher diffuse reflectance in between 400 nm and visible wavelength region than Normal films, which also confirms that the recycled lights at visible wavelength region are not absorbed by the TiO_2 nano particle materials, but also diffuse reflected by the micro-crater structure.

In order to investigate the effect of the thickness of the TiO_2 films against the light scattering properties, different thickness of TiO_2 films with and without AB were prepared using screen printing method by coating 1 time or 3 times repeatedly. The thickness were 8.2 μm and 19.3 μm by 1 time and 3 time coatings in Normal TiO_2 films, and 8.3 μm and 19.6 μm by 1 time or 3 times coatings in AB TiO_2 films, respectively. Micro-pores of AB based TiO_2 anodes are seen clearly between TiO_2 nanoparticles at SEM images in Figure 3. These pores were formed by the evaporation of AB at high temperature on TiO_2 nanoparticle film. The blending ratio of AB to TiO_2 paste before heat treatment was 1 wt. %. Micro-pores with mixed sizes ranging from several nanometers to several hundred nanometers were formed hierarchically on TiO_2 films along the channel established by the evaporation of AB at high temperature treatment.

Figure 4(a) shows the light transmittance, opacity, and haze values of the bare FTO glass, Normal TiO_2 film and AB TiO_2 film measured by the transmittance mode of the spectrophotometer. The light transmittances of the films decreased in proportional to the thickness or coating numbers, while exhibiting lower values in AB films compared to the Normal films. This phenomenon can be explained directly by the increase of diffuse reflectance of the Normal and AB TiO_2 films, and the diffuse reflectance and whiteness index values measured by the reflectance mode of the spectrophotometer are shown in Fig. 4 (b). From the data of the bare FTO glass, the opacity value by the transmittance mode of 14 % and the diffuse reflectance value by the reflectance mode of 27 %, we can understand that thin metal oxide layer on the transparent glass scatters or reflects the visible light fundamentally. In case of the Normal TiO_2 films, the thickness of the film was a very important parameter for the light scattering effect, exhibiting higher opacity, haze values in transmittance mode and higher diffuse reflectance, whiteness index values in reflectance mode. However, the thick films with nanoparticles have limit for an easy infiltration of the gel-type electrolyte. In case of the AB TiO_2 films, the thickness was not a major parameter for the light scattering effect, because the formation of the hierarchical micro-crater structure was a more effective parameter. By increasing the thickness of the AB films, the opacity, haze values were not changed much and the whiteness index value increased slightly. Therefore, it is clear that the AB TiO_2 films are more effective for light recycling with thin layer than Normal TiO_2 films and the hierarchical micro-crater structure can provide wide channels for easy infiltration of the electrolyte. The easy infiltration of the electrolyte is more important for the gel-type electrolyte having higher viscosity, which is essential to enhance the long-term stability of the DSSCs.

Photovoltaic evaluation results of the DSSCs using different types of electrolytes with AB TiO_2 photo-anode films are shown in Figure 5, and the photovoltaic parameters of each are indicated in table 1. (See Fig. 2 and Table 1 of the reference article 18 for the performance of DSSCs using Normal TiO_2 photo-anode films for different electrolyte types.) The enhancement of photo-conversion efficiency by using AB process was confirmed by all the different electrolyte types. When the photovoltaic parameters were compared with a DSSC using conventional liquid-type electrolyte, short-circuit current density of a DSSC using UV cured polymer gel type electrolyte is lower, due to the low ionic mobility in a viscous medium at room temperature despite its merit of the long-term stability and rather higher photovoltaic performance at high temperature. [17] However, the DSSCs using double layer gel type electrolyte with additional nano-gel type electrolyte on the UV cured polymer gel type electrolyte have shown analogous level of photo-conversion efficiency to the DSSC using high performance liquid-type electrolyte with similar short-circuit current density and higher open circuit voltage while maintaining long-term stability of the UV cured gel type electrolyte. This is because of the improved charge transfer rate between the electrolyte and counter electrode although the thickness of the gel-type electrolyte has become even thicker.

Incident-photo-to-current efficiencies (IPCEs) were compared between the DSSCs with Normal films and AB films commonly using double layer gel-type electrolyte and the results are shown in Figure 6. The IPCEs of the DSSCs using AB TiO_2 photo-anode films were increased in longer visible wavelength regions from 500 nm to 750 nm due to the effect of light recycling in the TiO_2 photo-anode films compared to the DSSCs using Normal TiO_2 photo-anode films without light scattering layer. This is a typical result indicating that the improved photo-conversion efficiency comes from light scattering effect and have a merit of utilization of longer visible wavelength regions.

The stability of the DSSCs incorporating the AB TiO_2 photo-anode film and a double layer gel-type electrolyte under continuous light illumination conditions were tested and the results are shown in Figure 7. As a representative parameter indicating the long-term stability, photo-conversion efficiencies of the DSSCs using double layer gel-type electrolyte were maintained well until the end of 300 hours test. This result means that the contact between the TiO_2 films and the electrolytes are maintained and sensitized dyes are not segregated until the measured time.

Conclusions

In summary, we demonstrated the control of morphology and optical properties of the TiO_2 photo-anode films by simply adding high temperature volatile material in the TiO_2 paste without using cumbersome hard or soft template. As a result, the light scattering effect and the infiltration process of gel-type

electrolyte could be improved. We investigated for the optimal heat treatment condition in which complete evaporation of AB was facilitated for the formation of micro-crater structure, and improved the optical properties such as opacity, haze and whiteness index values. On the contrary, the excess heat treatment condition resulted in the shrinkage of micro-porous morphology. In this study, the performance of the DSSCs with double layer gel-type electrolyte was enhanced to the level of 8.7 % from 7.9 % by using AB TiO_2 film through the optimization of optical properties without using any additional light scattering layer. Furthermore, the facile process of electrolyte infiltration by this method is considered to be a great prospect for large scale commercialization of quasi-solid state DSSCs in the near future.

Acknowledgements

This work was supported by Basic Research Program (2011-0018113), Global Frontier Research Center for Advanced Soft Electronics (2011-0031635) of National Research Fund (NRF) funded by Korea government (MEST), and the International Collaborative R&D Program of the Korea Institute of Energy Technology Evaluation and Planning (KETEP) grant funded by Ministry of Knowledge Economy of Korea government (2011-8520010020).

Notes and references

[a] Program in Nano Science and Technology, Graduate School of Convergence Science and Technology, Seoul National University, Seoul, 151-744, Republic of Korea
[b] Photovoltaic Research Center, Korea Institute of Energy Research, Daejeon, 305-343, Republic of Korea
[c] Advanced Institutes of Convergence Technology, Suwon, 443-270, Republic of Korea

1. M. Wang, X. Pan, X. Fang, L. Guo, C. Zhang, Y. Huang, Z. Huo and S. Dai, *Journal of Power Sources*, 2011, **196**, 5784-5791.
2. H.-E. Wang, L.-X. Zheng, C.-P. Liu, Y.-K. Liu, C.-Y. Luan, H. Cheng, Y. Y. Li, L. Martinu, J. A. Zapien and I. Bello, *The Journal of Physical Chemistry C*, 2011, **115**, 10419-10425.
3. A. Yella, H. W. Lee, H. N. Tsao, C. Yi, A. K. Chandiran, M. K. Nazeeruddin, E. W. Diau, C. Y. Yeh, S. M. Zakeeruddin and M. Gratzel, *Science*, 2011, **334**, 629-634.
4. J. Burschka, N. Pellet, S. J. Moon, R. Humphry-Baker, P. Gao, M. K. Nazeeruddin and M. Gratzel, *Nature*, 2013, **499**, 316-319.
5. K. Y. Cheung, C. T. Yip, A. B. Djurišić, Y. H. Leung and W. K. Chan, *Advanced Functional Materials*, 2007, **17**, 555-562.
6. J. Liu, H. Yang, W. Tan, X. Zhou and Y. Lin, *Electrochimica Acta*, 2010, **56**, 396-400.
7. Y. Duan, N. Fu, Q. Liu, Y. Fang, X. Zhou, J. Zhang and Y. Lin, *The Journal of Physical Chemistry C*, 2012, **116**, 8888-8893.
8. M. K. Aminian, N. Taghavinia, A. Iraji-Zad, S. Mahdavi, M. Chavoshi and S. Ahmadian, *Nanotechnology*, 2006, **17**, 520.
9. Z. Liu, Z. Jin, X. Liu, Y. Fu and G. Liu, *Journal of sol-gel science and technology*, 2006, **38**, 73-78.
10. D. Chen, F. Huang, Y. B. Cheng and R. A. Caruso, *Advanced Materials*, 2009, **21**, 2206-2210.
11. G. Hasegawa, K. Kanamori, K. Nakanishi and T. Hanada, *Journal of the American Ceramic Society*, 2010, **93**, 3110-3115.
12. C. Y. Cho and J. H. Moon, *Advanced Materials*, 2011, **23**, 2971-2975.
13. Q. L. Wu, N. Subramanian and S. E. Rankin, *Langmuir*, 2011, **27**, 9557-9566.
14. G. Cheng, M. S. Akhtar, O. B. Yang and F. J. Stadler, *Electrochimica Acta*, 2013, **113**, 527-535.
15. S. J. Park, K. Yoo, J. Y. Kim, J. Y. Kim, D. K. Lee, B. Kim, H. Kim, J. H. Kim, J. Cho and M. J. Ko, *ACS Nano*, 2013, **7**, 4050-4056.
16. T. Kato, A. Okazaki and S. Hayase, *J. Photochem. Photobiol. A-Chem.*, 2006, **179**, 42-48.
17. H.-S. Lee, C.-H. Han, Y.-M. Sung, S. S. Sekhon and K.-J. Kim, *Current Applied Physics*, 2011, **11**, S158-S162.
18. D. M. Han, K.-W. Ko, C.-H. Han and Y. S. Kim, *Journal of Materials Chemistry A*, 2013, **1**, 8529.
19. J. W. Jinshu Wang, Hongyi Li, *Material Matters*, 2012, **7**, 2-6.
20. T. Y. Cho, C. W. Han, Y. Jun and S. G. Yoon, *Scientific reports*, 2013, **3**, 1496.

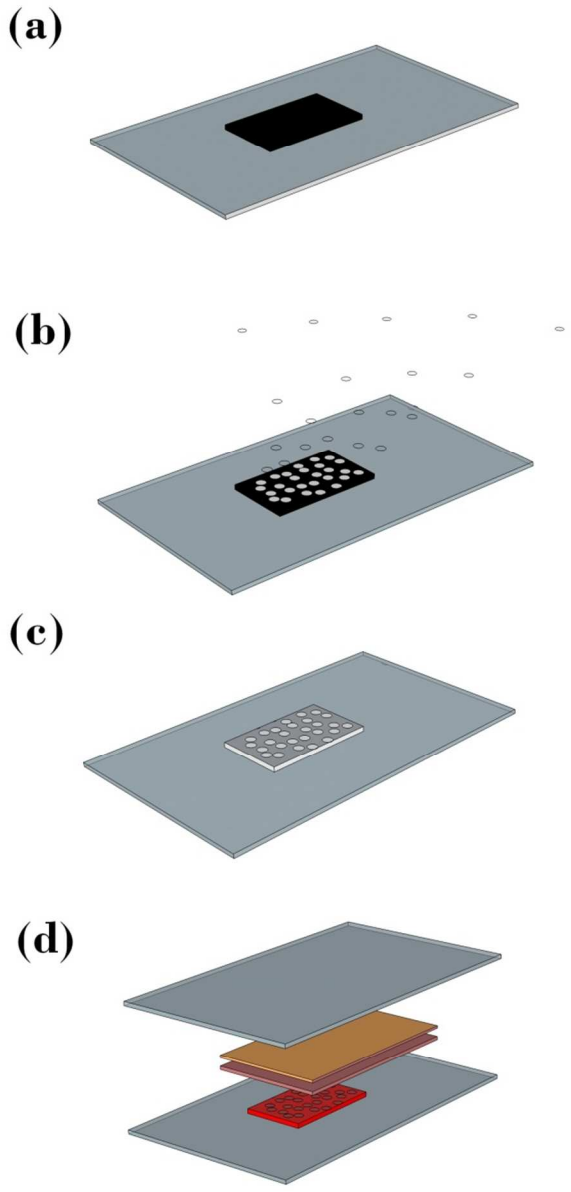

Scheme 1 Novel fabrication process using TiO_2 photo-anode film with acetylene-black for double layer gel-type electrolyte DSSC (a) TiO_2 film on FTO glass (b) evaporation of acetylene-black at high temperature treatment (c) hierarchical micro porous structure formation and (d) fabrication of double layer gel-type electrolyte between the the two electrode glasses

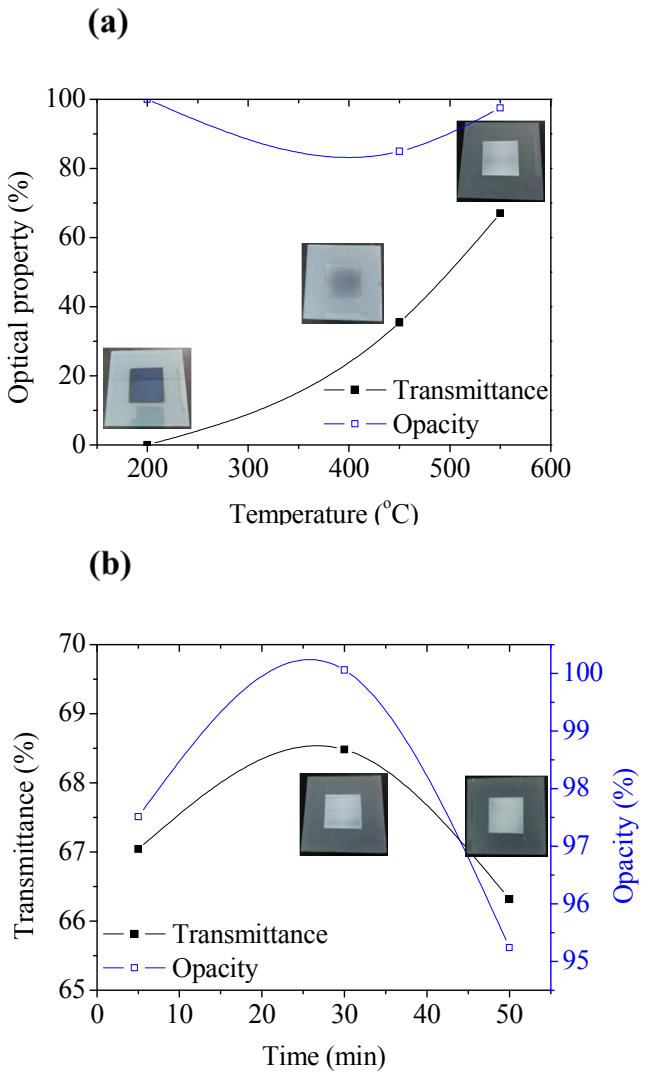

Fig. 1 Optical properties of the TiO_2 photo-anode films containing 1 wt% of acetylene-black measured by spectrophotometer according to (a) The heat treatment conditions of 200 °C for 60 minutes, 450 °C for 60 minutes, and 550 °C for 5 minutes, and (b) The heat treatment times of 5 minutes, 30 minutes, and 50 minutes at 550 °C. Each photograph images indicated inset correspond to each measured points.

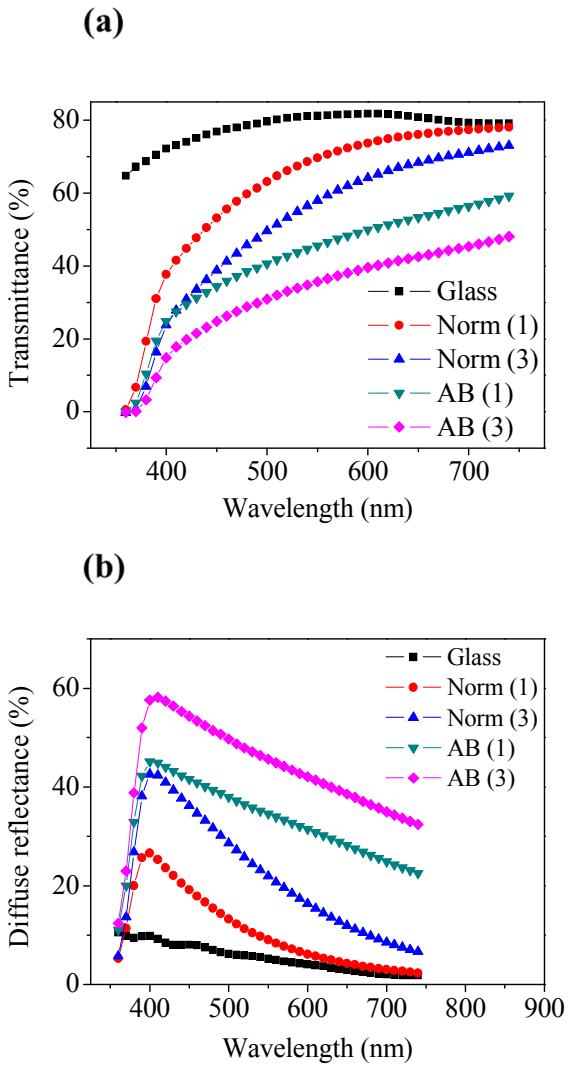

Fig. 2 Comparison of the (a) Transmittances and (b) Reflectances of the TiO_2 photo-anode films prepared as bare FTO glass, normal TiO_2 film screen printed one time or three times, AB TiO_2 film screen printed one time or three times, respectively. Here, A.B. denotes the acetylene-black.

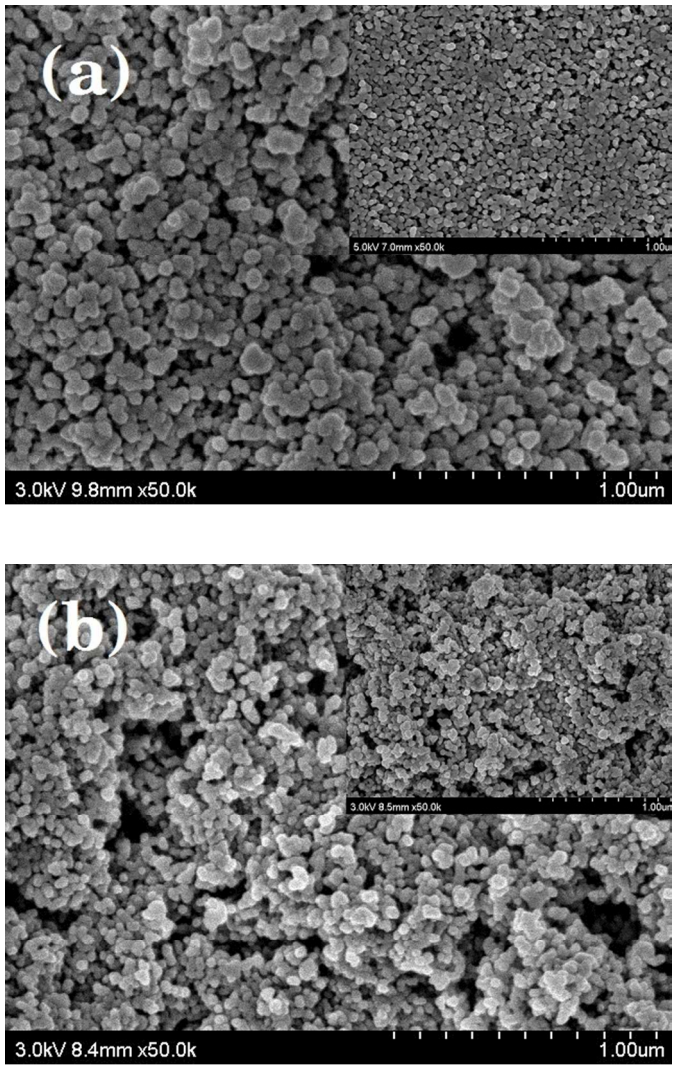

Fig. 3 Scanning electron micrograph images of (a) Normal TiO_2 photo-anode film and (b) AB TiO_2 photo-anode film. Inset images are cross-section view images, respectively.

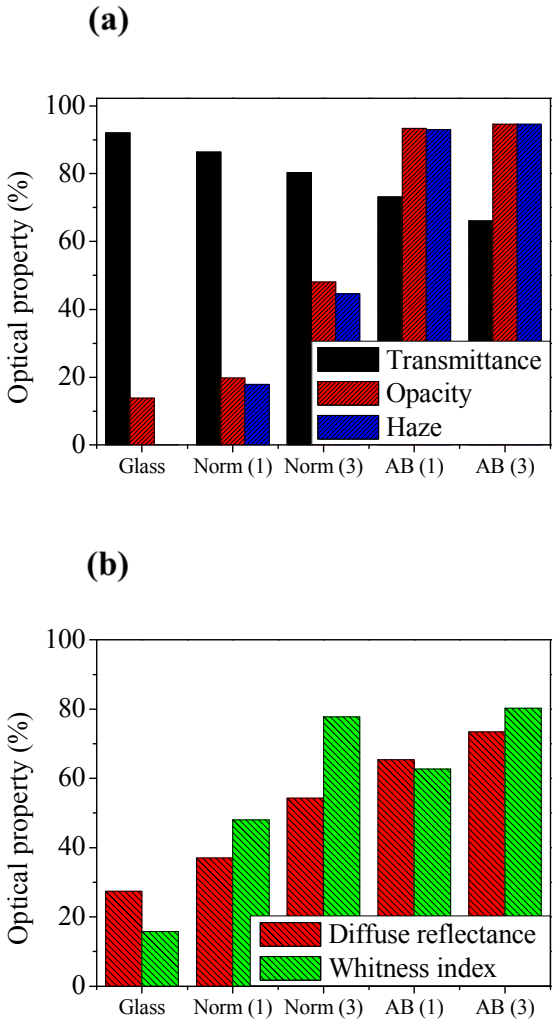

Fig. 4 Comparison of the various optical properties according to the thickness measured by (a) Transmittance mode and (b) Diffuse reflectance mode of the bare FTO glass, normal TiO_2 films, and AB TiO_2 films which were screen printed one time or three times, respectively.

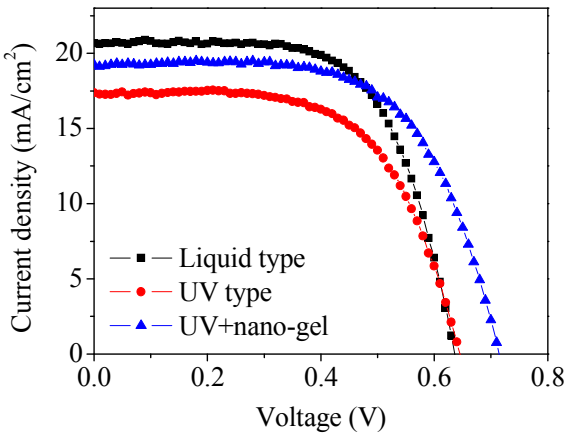

Fig. 5 Current density-voltage (*J–V*) curves of the DSSCs fabricated using different types of electrolytes as liquid-type, UV-cured polymer gel type, and double layer gel-type on the AB TiO_2 photo-anode films, measured by solar simulator under 1 sun, AM 1.5G condition.

Table 1 Photovoltaic parameters of the DSSCs fabricated using different types of electrolytes as liquid type, UV-cured polymer gel type, and double layer gel-type on the AB TiO2 films, and measured by solar simulator under 1 sun, AM 1.5G condition.

Electrolytes	J_{SC}(mA/cm^2)	V_{OC}(V)	Fill Factor	η(%)
Liquid type	20.673	0.636	0.645	8.492
UV type	17.385	0.645	0.616	6.918
UV + nano-gel	19.242	0.714	0.634	8.721

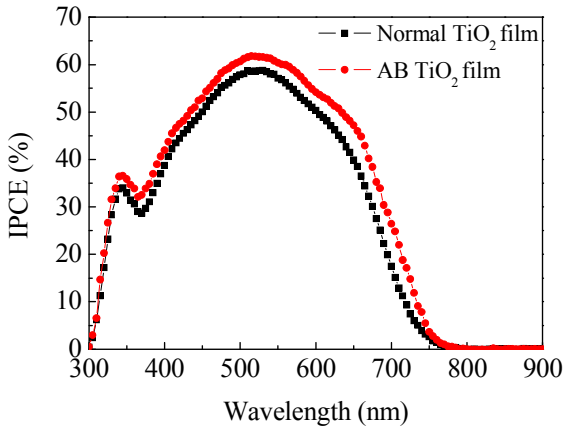

Fig. 6 Incident-photo-to-current efficiencies (IPCEs) measurement of the DSSCs using normal TiO_2 photo-anode films or AB TiO_2 photo-anode films commonly with double layer gel-type electrolyte.

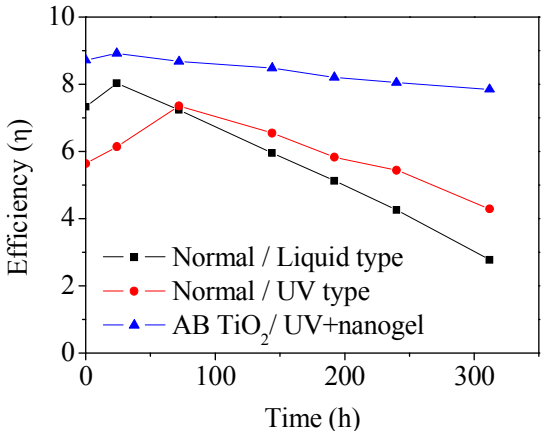

Fig. 7 Stability test result of the DSSC using double layer gel-type electrolyte with AB TiO_2 photo-anode film compared with DSSCs using Liquid type or UV type electrolyte with Normal TiO_2 photo-anode film measured by solar simulator under continuous light illumination at ambient temperature.

Facile formation of micro-crater structure for light scattering in quasi-solid state dye-sensitized solar cells

Dae Man Han,[a] Kwan-Woo Ko,[b] Chi-Whan Han [*b] and Youn Sang Kim [*ac]

The formation of micro-crater structure with optimal morphology in dye-sensitized solar cell (DSSC) improved the light scattering effect without additional light scattering layer, in addition, provided wide entrance for fast and complete electrolyte infiltration into the TiO_2 film. Photo-conversion efficiency of the DSSC using this method was enhanced from 7.9 % to 8.7 %, while maintaining a high stable efficiency in 300 hours stability test.